The benzoylurea derivative F13 inhibits cell growth, migration and invasion through inducing expression of ERK1/2-mediated RECK in fibrosarcoma HT-1080 cells

Haixia Jin[a,b], Kaihuan Ren[a], Hong-Wei He[a], Xia Liu[a], Dan-Qing Song[c] and Rong-Guang Shao[a]

3-Bromoacetamino-4-methoxy-benzoylurea (F13) is a benzoylurea derivative selected from the library of small molecule tubulin ligands. Our earlier data showed that F13 had lost the capacity to interrupt microtubule dynamics while reserving anticancer activity. In this study, we found that F13 greatly inhibited cell proliferation in various human cancer cells. At concentrations of more than 1 μg/ml, F13 markedly slowed growth and induced apoptosis in HT-1080 cells. This apoptosis occurred through cleavages of caspase 3 and PARP. At low concentrations (≤ 1 μg/ml), F13 reduced the migration, adhesion, and invasion of HT-1080 cells. In addition, F13 downregulated the activities of matrix metalloproteinase-2/9 (MMP-2/9) in a culture supernatant. This was found to occur through the upregulation of the reversion-inducing cysteine-rich protein with Kazal motifs (RECK), a membrane-anchored inhibitor of MMPs, which acts by reducing ERK1/2 phosphorylation. Our data suggested that F13 might act as a novel RECK inducer, inhibiting cancerous processes with the inactivation of MMP-2/9 by the induction of RECK through the inhibition of ERK1/2 signalling transduction. *Anti-Cancer Drugs* 21:372–380 © 2010 Wolters Kluwer Health | Lippincott Williams & Wilkins.

Anti-Cancer Drugs 2010, **21**:372–380

Keywords: apoptosis, benzoylurea derivative, fibrosarcoma HT-1080, metastasis, RECK

Departments of [a]Oncology, [b]Pharmacology, Beijing Tuberculosis and Thoracic Tumor Research Institute and [c]Chemical Biology, Institute of Medicinal Biotechnology, Peking Union Medical College, Chinese Academy of Medical Sciences, Beijing, China

Correspondence to Rong-Guang Shao, Department of Oncology, Institute of Medicinal Biotechnology, Peking Union Medical College, Chinese Academy of Medical Sciences, 1 Tiantan Xili, Beijing 100050, China
Tel: +86 10 63026956; fax: +86 10 63017302;
e-mail: shaor@bbn.cn; songdanqingsdq@hotmail.com

Received 21 July 2009 **Revised form accepted** 18 November 2009

Introduction

Cancer remains a leading cause of death throughout the world. Although mortality rates have declined in recent years because of earlier detection and the availability of new treatment options, most cancers remain incurable [1]. Although chemotherapy has been used mainly against the primary tumor, there is no effective therapy available for metastatic cancer after surgery, or radiation [2]. Therefore, the search for promising agents that disturb tumor growth and metastasis is one of the most popular research topics for cancer therapy. Up to now, a few highly active antitumor agents, such as the anticancer antibiotic lidamycin and dietary compound, curcumin, which are both in clinical trials, have emerged and attracted considerable attention because of their strong activities against cancer cell growth and metastasis [3,4]. As a potent chemotherapeutic agent, lidamycin causes cellular DNA damage and induces apoptosis and mitotic cell death at high concentrations [5–10], and blocks cell cycle progress, inhibits metastasis, invasion, and angiogenesis at low concentrations [11–14]. Curcumin also induces cell apoptosis and reduces cell viability at high concentrations and significantly inhibits cell migration and invasion at low concentrations [4,15].

Microtubule dynamics have been identified as a rational site to interfere with the division of cancer cells. Tubulin ligands that target the dynamic process induce mitotic arrest in the cell cycle [16–18]. Such compounds have been used in the clinic for cancer chemotherapy (Vinca alkaloids, podophyllotoxin, and taxanes). Earlier, to construct a library of small molecule tubulin ligands, a number of 3-haloacylamino benzoylureas had been designed, synthesized, and evaluated [19–21]. Some of the compounds have shown anticancer activity *in vitro* and *in vivo* and become a new family of tubulin ligands [22–24]. Among the analogues, 3-bromoacetamino-4-methoxy-benzoylurea (F13) (Fig. 1) bears an OCH_3 substituent at the 4-position of the phenyl ring, losing the capacity to interrupt microtubule dynamics while reserving anticancer activity equal to the parent compound [20,24]. In this study, we further investigated the efficiency and mechanisms of F13's effect on human cancer cells. We observed that F13 markedly inhibited cell proliferation in a panel of seven human cancer cell lines. Our data showed, for the first time, that F13 dose-dependently inhibited growth, migration, adhesion and invasion of fibrosarcoma HT-1080 cells and induced apoptotic cell death. The changes in signalling molecules such as caspase 3, PARP, ERK1/2, RECK and matrix metalloproteinase (MMP) were also determined.

Materials and methods

Reagents

F13 was synthesized in our laboratory as described earlier [20]. It has a molecular weight of 329 Da, and

0959-4973 © 2010 Wolters Kluwer Health | Lippincott Williams & Wilkins DOI: 10.1097/CAD.0b013e3283357c44

Fig. 1

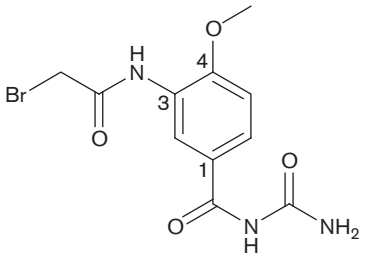

Chemical structure of 3-bromoacetamino-4-methoxy-benzoylurea (F13).

the structure as shown in Fig. 1 was confirmed by mass spectrometry and proton nuclear magnetic resonance spectroscopy. A 20 mg/ml stock solution was prepared in dimethylsulphoxide and was diluted in a medium before use. Equal volumes of solvents were used as controls. U0126 (Sigma, Saint Louis, Missouri, USA) was dissolved in dimethylsulphoxide and diluted in the medium.

Cell lines

Cell lines listed in Table 1 were from American Type Culture Collection except human hepatoma BEL-7402 cells (Institute of Biochemistry and Cell Biology, Chinese Academy of Sciences, Shanghai, China). Hep G_2 cells and HT-1080 cells were grown in the minimum essential medium Eagles with Earle's balanced salts (MEM-EBSS) medium (Hyclone, Logan, Utah, USA). MCF7 cells and HCT116 cells were grown in the Dulbecco's minimum essential medium (Hyclone). All the other cells were grown in the RPMI 1640 medium (Hyclone). The medium was supplemented with 100 U/ml penicillin and 100 μg/ml streptomycin and 10% fetal bovine serum (FBS) at 37°C in a humidified atmosphere containing 5% CO_2.

Determination of IC_{50} values

Cells were seeded into 96-well microplates at 1.0×10^4/well, followed by treatment with F13 at concentrations between 0 and 10 μg/ml for 24 h at 37°C. Cell viability was assessed by MTT staining [25]. Cancericidal activity was determined in duplicate, and each experiment was repeated three times under identical conditions. The IC_{50} was defined as the drug concentration that induced 50% cellular death in comparison with untreated controls and was calculated by nonlinear regression analyses.

Cell proliferation assay

The cells were treated with the indicated concentrations of F13 for 24 h and collected. Five milliliters of cells were seeded at a density of 6000/ml in a 25 cm^2 cell culture flask with a 10% FBS medium. The medium was changed regularly. The cell number was counted every 24 h for 7 days.

Table 1 Antiproliferative activity of F13 in various tumor cell lines

Cell line	IC_{50} (μg/ml)
Human fibrosarcoma HT-1080	2.515 ± 0.175
Human breast cancer MCF7	3.144 ± 0.098
Human colon carcinoma HT-29	1.110 ± 0.076
Human colon carcinoma HCT 116	1.922 ± 0.126
Human lung cancer A549	4.149 ± 0.124
Human hepatoma Hep G_2	2.680 ± 0.137
Human hepatoma BEL-7402	3.139 ± 0.195
Human normal liver L02	4.653 ± 0.315

Values are mean ± SD, $n = 3$; evaluated by MTT assay.
F13, 3-bromoacetamino-4-methoxy-benzoylurea.

Cell cycle analysis

The cells were treated as indicated. Floating and adherent cells were collected by centrifugation. The cells were fixed in 80% ethanol for 24 h at −20°C, washed with phosphate-buffered saline (PBS) and stained with PBS containing 50 μg/ml propidium iodide (PI) and 200 μg/ml RNase A for 30 min. Analyses were performed with flow cytometry (FACSCalibur, BD Bioscience, San Jose, California, USA).

Annexin-V/propidium iodide staining and terminal deoxyribonucleotide transferase-mediated dUTP nick end-labeling assays

To determine the percentage of apoptotic cells, the cells were treated as indicated, and phosphatidylserine cell translocation and plasma membrane permeability were evaluated by dual staining with fluorescein isothiocyanate-conjugated Annexin-V and PI, using the Annexin-V/PI apoptosis detection kit (Roche, Mannheim, Germany), and analyzed by FACSCalibur flow cytometry. For the terminal deoxyribonucleotide transferase-mediated dUTP nick end-labeling (TUNEL) assay, the cells were treated as indicated and TUNEL staining was performed *in situ* using the DeadEnd fluorometric TUNEL system kit (Promega, Madison, Wisconsin, USA) according to the manufacturer's protocol. The images were captured by an image analysis system (Eclipse TE2000-U, Nikon, Japan).

Wound-healing assay

Cells were cultured in 24-well plates and grown in a medium containing 10% FBS to a nearly confluent cell monolayer, then carefully scratched using a plastic pipette tip to draw a linear 'wound' in the cell monolayer of each well. The monolayer was washed twice with PBS to remove debris or the detached cells from the monolayer, and then treated with F13 for the indicated concentrations monitored by the Eclipse TE2000-U image analysis system. The experiments were performed in triplicate.

Transwell migration assay

Briefly, Transwell filters (8-μm pores, Costar, Cambridge, Massachusetts, USA) were used. Cells suspended in serum-free MEM-EBSS containing 0.1% bovine serum

albumin (BSA) and the indicated concentrations of F13, were applied to the upper chamber (20 000 cells per well). To the lower wells of the chambers, MEM-EBSS containing 20% FBS and 10 μg/ml fibronectin (FN) was added. After 6 h incubation at 37°C, assays were stopped by removal of the medium from the upper wells and careful removal of the filters. The filters were fixed with methanol by brief submersion and cells on the upper side were wiped off. Filters were stained with hematoxylin and random fields were scanned (five fields per filter) under a light microscope (magnification, ×400) for the presence of cells at the lower membrane side only.

Matrigel-based Transwell invasion assay

Briefly, Transwell filters (8-μm pores, Costar) coated with 2.5 mg/ml Matrigel (BD Biosciences, Bedford, Massachusetts, USA) were used. Cells (10^5 per well) suspended in serum-free MEM-EBSS containing 0.1% BSA and indicated concentrations of F13 were seeded onto the upper chambers of the precoated transwells. To the lower wells of the chambers, MEM-EBSS containing 20% FBS and 10 μg/ml FN was added. After 12 h incubation, cells on the upper well were wiped off and the membranes were fixed and stained. Cells that were attached to the lower surface of the polycarbonate filter were counted under a light microscope (magnification, ×400).

Cell adhesion assay

Cells were washed in serum-free MEM-EBSS and resuspended in a culture medium with the indicated concentrations of F13. One hundred microliters of suspended cells were added to each well of 96-well plates coated with 10 μg/ml FN and blocked with 1 μg/ml BSA. The plates were incubated for indicated periods of time at 37°C in a CO_2 incubator. Non-adherent cells were removed by washing with PBS, and the attached cells were analyzed by the MTT assay.

Zymography

The activities of MMP-2/9 in the culture-conditioned medium were assayed by gelatin zymography [26]. Cells (10^5 cells/well) were seeded into 24-well plates and maintained for 24 h in MEM-EBSS with 10% FBS. Subconfluent cells were incubated for 24 h at the indicated concentrations of F13 in serum-free MEM-EBSS, and culture supernatants were collected from equal numbers of cells. Without heating and under nonreducing conditions, the samples were subjected to electrophoresis in 0.1% w/v gelatin-containing 10% polyacrylamide gel in the presence of sodium dodecyl sulfate. After electrophoresis, the gel was washed twice for 30 min in 2.5% Triton X 100 and incubated for 18 h at 37°C in Tris buffer (50 mmol/l Tris–HCl, 200 mmol/l NaCl, and 10 mmol/l $CaCl_2$, pH 7.4). The gels were stained with Coomassie brilliant blue R (0.1% w/v) and de-stained in a solution of 30% methanol and 10% acetic acid. Gelatinolytic activity appeared as a clear band on a blue background.

Reverse transcription-polymerase chain reaction

Total mRNA was extracted from the cells by Trizol reagent (Invitrogen, Carlsbad, California, USA) with an extra step of acid phenol extraction. Reverse transcription-polymerase chain reaction (RT-PCR) was carried out using a SuperScript One-step RT-PCR kit (Invitrogen) as described earlier [27]. The oligonucleotide primers used were as follows: RECK Primer1 (P1), 5′-CCT CAG TGA GCA CAG TTC AGA-3′; RECK Primer2 (P2), 5′-GCA GCA CAC ACA CTG CTG TA-3′; glyceraldehyde-3-phosphate dehydrogenase (GAPDH) P1, 5′-CCC ATC ACC ATC TTC CAG-3′; GAPDH P2, 5′-CAG TCT TCT GGG TGG CAG T-3′. GAPDH mRNA was analyzed as an internal control. A measure of 1 μg of total RNA was reverse transcribed to synthesize cDNA at 50°C for 45 min, and then the cDNA was subjected to PCR amplification with specific primers in 25 μl mixtures. PCR comprised 40 cycles with denaturing at 94°C for 15 s, annealing at 60°C for 30 s and extension at 72°C for 1 min in each cycle using an MJ PCR System. PCR products were separated on a *2%* of 0.5 × Tris-borate EDTA agarose gel.

Quantitative real time reverse transcription-polymerase chain reaction

Quantitative real time reverse transcription-polymerase chain reaction (qRT-PCR) was performed using specific sense and antisense primers in a 25 μl reaction volume containing 12.5 μl Absolute QPCR SYBR Green Mix (Invitrogen), 0.25 pmol of each primer and 0.5 μg mRNA. Oligonucleotide primers used as follows: for MMP-*2* P1, 5′-ATA ACC TGG ATG CCG TCG T-3′; MMP-*2* P2, 5′-AGG CAC CCT TGA AGA AGT AGC-3′; MMP-9 P1, 5′-GAA CCA ATC TCA CCG ACA GG-3′; MMP-9 P2, 5′-GCC ACC CGA GTG TAA CCA TA-3′; GAPDH P1, 5′-TCC ACT GGC GTC TTC ACC-3′; GAPDH P2, 5′-GGC AGA GAT GAT GAC CCT TTT-3′. The cycling conditions were initial denaturation at 50°C for 3 min, 95°C for 5 min, and 40 cycles at 95°C for 15 s, 60°C for 30 s.

Western blot

Cells were washed twice in cold PBS and then lysed in a lysis buffer (50 mmol/l Tris–HCl pH 7.5; 1% NP-40; 150 mmol/l NaCl; 1 mg/ml aprotinin; 1 mg/ml leupeptin; 1 mmol/l Na_3VO_4; 1 mmol/l NaF) at 4°C for 30 min. Cell debris was removed by centrifugation at 14 000 *g* for 20 min at 4°C. Protein concentrations were determined by the Bradford assay as described in the standard protocol [28]. Cell lysates were separated on 10–12% sodium dodecyl sulfate polyacrylamide gels, transfered to polyvinylidene fluoride membranes (Millipore, Bedford, Massachusetts, USA) and immunoblotted with specific antibodies as well as horseradish peroxidase-conjugated appropriate secondary antibodies. β-Actin was used as a loading control. The antibodies used were anti-ERK1/2 and anti-phospho-ERK1/2 (Thr202/Tyr204) (Cell Signaling Technology, Beverley, Massachusetts, USA), anti-caspase 3,

anti-PARP, and anti-β-actin (Santa Cruz Biotechnology, California, USA) and horseradish peroxidase-conjugated goat anti-mouse or goat anti-rabbit secondary antibody (Jackson Inc., West Grove, Pennsylvania, USA). Electrochemiluminescence was performed according to the manufacturer's instructions with ChemiImager 5500 imaging system (Alpha Innotech Corporation, San Leandro, California, USA).

Statistical analysis

Data were described as the arithmetic mean ± SD. Statistical analysis was performed using Student's *t*-test. A *P* value of less than 0.05 was considered statistically significant.

Results

F13 inhibited the growth of various human cancer cells

As shown in Table 1, the MTT assay showed that F13 significantly inhibited cell proliferation in seven cancer cell lines representing five types of cancers, including fibrosarcoma, hepatoma, colon carcinoma, breast and lung cancer. The IC_{50} values of F13 were in the range of approximately 1.11–4.15 μg/ml for various human cancer cells and 4.65 μg/ml for human normal liver L02 cells. The most sensitive cells tested in this study were HT-29 cells, which were 4-fold more susceptible in comparison with L02 cells.

The highly mobile fibrosarcoma HT-1080 cells were also sensitive to F13, and its IC_{50} value was 2.51 μg/ml. To investigate the effects of F13 on cell growth, migration, adhesion and invasion, human fibrosarcoma HT-1080 cells were used in the following experiments. After treatment, we observed that F13 inhibited the proliferation of HT-1080 cells in time-dependent and dose-dependent manners (Fig. 2). At concentrations of approximately 2.5–5 μg/ml, F13 markedly inhibited cell growth; however, there was no significant effect compared with control, until day 6 when F13 was given at approximately 0.5–1 μg/ml.

F13-induced apoptosis in HT-1080 cells

Our earlier data have shown that F13 had lost the capacity to interrupt microtubule dynamics. In this study, we investigated the effect of F13 on cell cycle progression. HT-1080 cells were treated with different concentrations of F13 for 24 h and then cell cycle distribution was determined. Flow cytometry showed that F13 treatment did not obviously affect cell cycle distribution (Fig. 3), consistent with our earlier data. After 48 h exposure to F13, the cell cycle distribution was also not changed. At 72 h treatment, most of the cells underwent apoptosis (data not shown).

Annexin-V/PI staining revealed that HT-1080 cells treated with approximately 2.5–5 μg/ml F13 resulted in

Fig. 2

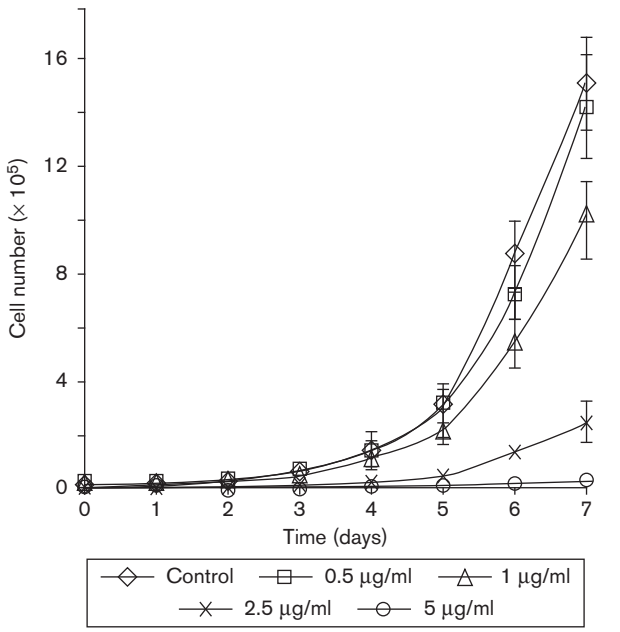

3-Bromoacetamino-4-methoxy-benzoylurea inhibits the growth of HT-1080 cells. The cells were treated with the various concentrations of 3-bromoacetamino-4-methoxy-benzoylurea for the indicated times. Data are mean ± SD of three independent experiments.

Fig. 3

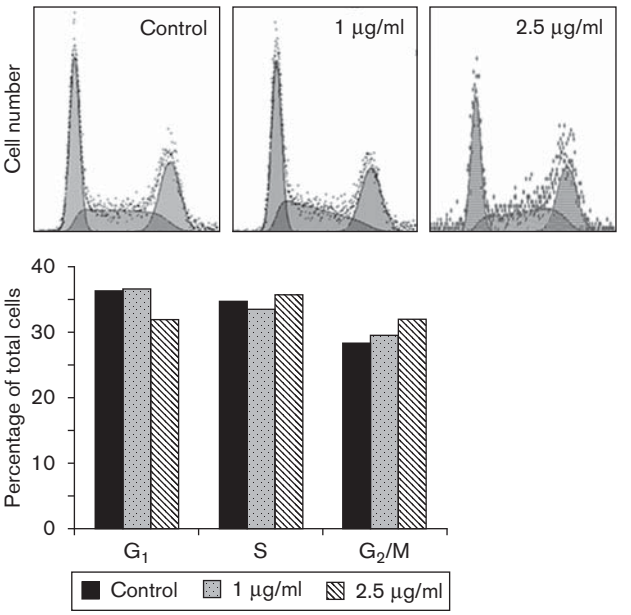

3-Bromoacetamino-4-methoxy-benzoylurea has no obvious effect on HT-1080 cell cycle distribution. Cells were treated with the indicated concentrations of 3-bromoacetamino-4-methoxy-benzoylurea for 24 h and cell cycle distribution was examined as described in the Materials and methods section.

Fig. 4

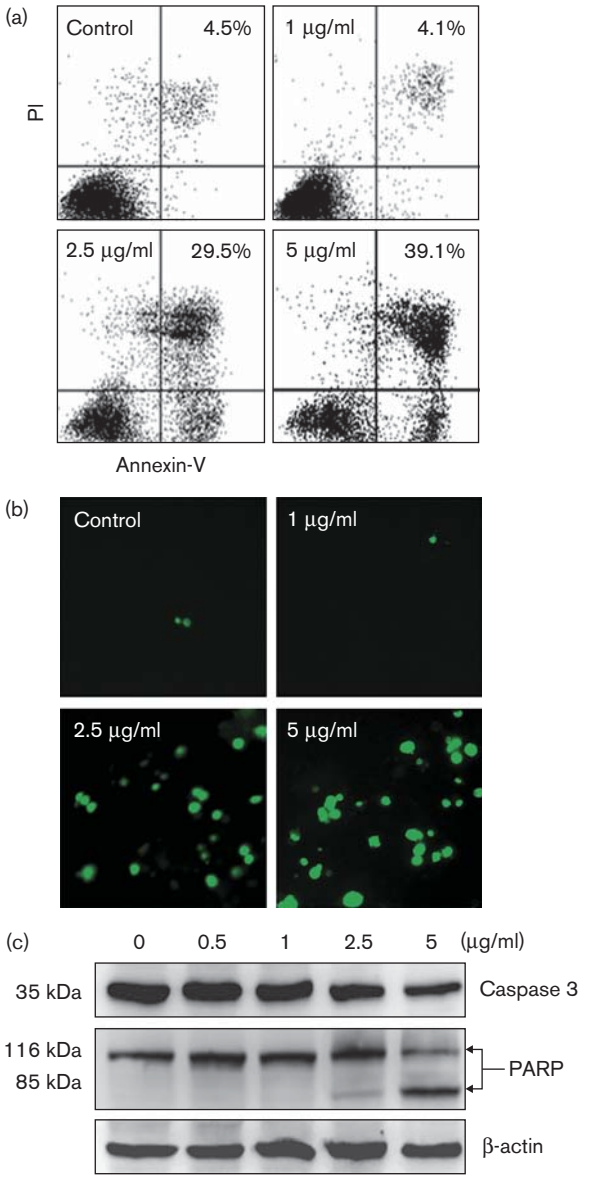

The 3-bromoacetamino-4-methoxy-benzoylurea-induced apoptosis in HT-1080 cells. Cells were treated by 3-bromoacetamino-4-methoxy-benzoylurea at the indicated concentrations for 24 h, and analyzed by Annexin-V/PI staining (a) and TUNEL fluorescence staining (b). Caspase 3 and PARP were detected by western blot (c). β-Actin served as a loading control.

a significant increase in apoptosis in a dose-dependent manner (Fig. 4a). The percentage of early apoptotic cells (Annexin-V positive/PI negative) for 2.5 and 5 μg/ml was increased from 0.9% to 14.7% and 15.6%, respectively, and the percentage of late apoptotic cells or necrotic cells (Annexin-V positive/PI positive) for 2.5 and 5 μg/ml was increased from 4.5% to 29.5% and 39.1%, respectively. In contrast, no obvious apoptosis was induced by 1 μg/ml F13 compared with controls.

Fig. 5

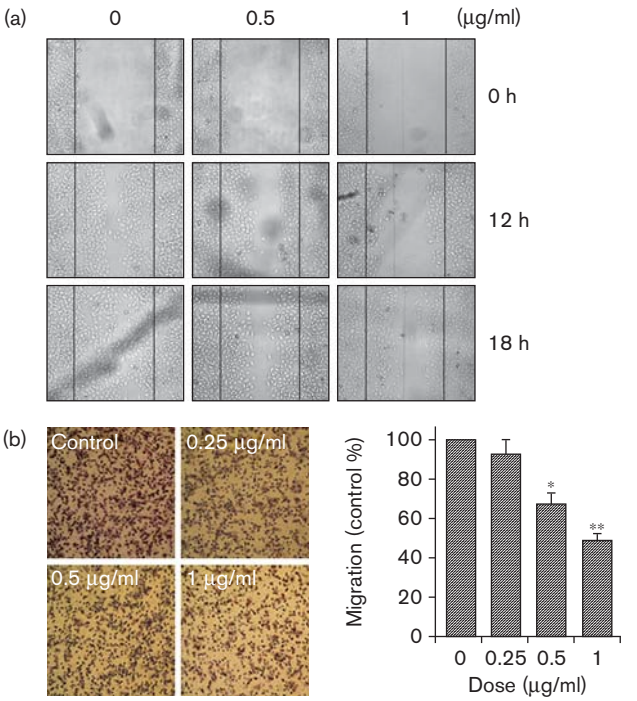

3-Bromoacetamino-4-methoxy-benzoylurea inhibits HT-1080 cell migration. Cells were treated with the indicated concentrations of 3-bromoacetamino-4-methoxy-benzoylurea and incubated for the indicated times then detected by the wound healing assay (a) and for 6 h by the Transwell migration assay (b). Data are mean ± SD of three independent experiments (*$P<0.05$; **$P<0.005$, compared with the control).

To further confirm that F13 could induce apoptosis in HT-1080 cells at concentrations more than 1 μg/ml, TUNEL staining was applied. As shown in Fig. 4b, at concentrations of approximately 2.5–5 μg/ml, F13 induced an increased frequency of apoptotic cells (green) after exposure for 24 h, whereas no obvious apoptotic cells were accumulated at the concentration of 1 μg/ml. These results suggested that at concentrations over 1 μg/ml, F13 could induce apoptosis. This effect was further shown by western blot as shown in Fig. 4c, the treatment of HT-1080 cells up to 2.5 μg/ml caused downregulation of caspase 3 protein level and consequent cleavage of PARP to its characteristic 85 kDa.

F13 inhibited the migration, invasion, and adhesion of HT-1080 cells

On account of the finding that F13 could reduce cell viability and induce cell apoptosis in HT-1080 cells at concentrations over 1 μg/ml, we investigated whether F13 inhibited cell migration, invasion, and adhesion at concentrations of ≤ 1 μg/ml. The results of the wound-healing assay and Transwell migration models showed that

Fig. 6

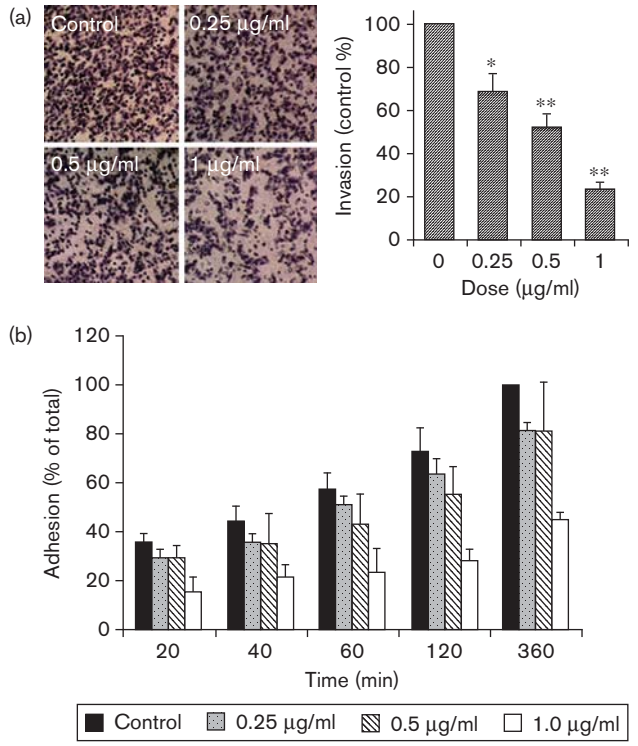

3-Bromoacetamino-4-methoxy-benzoylurea inhibits HT-1080 cell invasion and adhesion. (a) Cells were treated with the indicated concentrations of 3-bromoacetamino-4-methoxy-benzoylurea and incubated for 12 h then detected by the Matrigel Invasion Assay. (b) Cells were seeded in FN-coated 96-well plates and incubated at the indicated concentrations for the indicated times. Data are mean ± SD of three independent experiments (*$P<0.05$; **$P<0.005$, compared with control).

F13 was able dose-dependently (approximately 0.25–1 μg/ml) to significantly inhibit HT-1080 cell migration (Fig 5a and b). As shown in Fig. 5a, the number of cells migrating into the wound area was reduced in the presence of F13 compared with control. In some conditions, cells migrating into the lower side of the filter were reduced to 66.7 and 48.1% for 0.5 and 1 μg/ml, respectively (Fig. 5b).

In addition, the matrigel-based Transwell assay revealed that F13 was able to significantly inhibit cell invasion. Cells migrating through the matrigel into the lower side of the filter were significantly inhibited by F13 to 68.3, 52.1 and 23.3% of the control for 0.25, 0.5, and 1 μg/ml, respectively (Fig. 6a). Since cell adhesion to extracellular matrix (ECM) is a critical step of tumor cell invasion, we further determined the effect of F13 on HT-1080 cell adhesion to the ECM molecule FN. As shown in Fig. 6b, the adhesion of cells to FN was inhibited by F13 in a dose-dependent manner.

Fig. 7

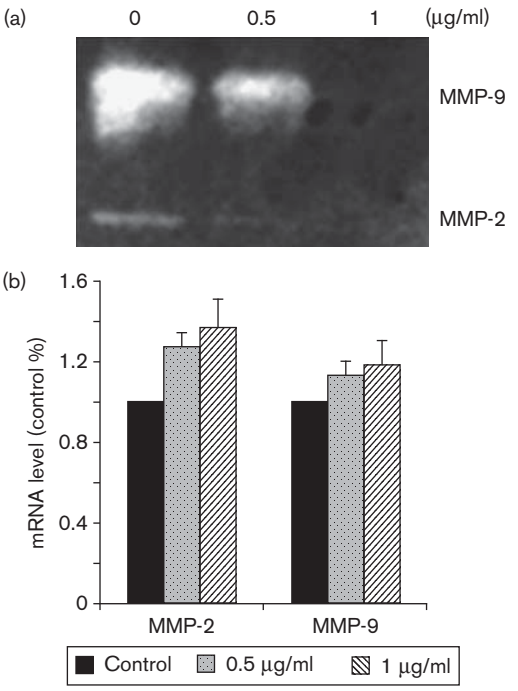

MMP-2/9 is inhibited by F13. Cells were treated with the indicated concentrations of F13 for 24 h. (a) Collagenase activities were determined by gelatin zymography. (b) The mRNA levels were detected by quantitative real time reverse transcription–polymerase chain reaction. Data are mean ± SD of three independent experiments. MMP, matrix metalloproteinase.

Activations of matrix metalloproteinase-2/9 were suppressed by F13

A key step in the invasive progress is the degradation of ECM by MMPs. Gelatinases MMP-2 and MMP-9 are considered to be the major proteolytic enzymes in the degradation of ECM during cancer cell progression and invasion. Gelatin zymography of MMPs revealed that the activities of MMP-9 and MMP-2 in the culture supernatant were downregulated by F13 with absolute suppression at 1 μg/ml (Fig. 7a).

To investigate whether the decrease of MMP-2/9 levels in the supernatant was because of reduced MMP-2/9 mRNA expression, qRT-PCR analysis was used. Interestingly, the expression of MMP-2/9 mRNA appeared to be slight increase (Fig. 7b). Taken together, our results suggested that the downregulations of MMP-2/9 activities might be a result of post-transcriptional events.

F13 upregulated expression of RECK through the inactivation of ERK1/2

We next examined the expression of the reversion-inducing cysteine-rich protein with Kazal motifs (RECK). RECK is a novel MMP inhibitor that was originally isolated as a transformation suppressor gene against the activated ras oncogene [29–31]. Earlier studies have

Fig. 8

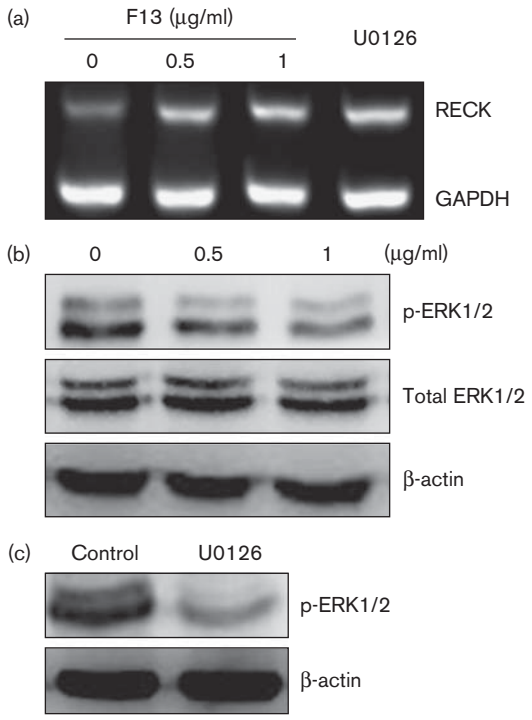

3-Bromoacetamino-4-methoxy-benzoylurea induces expression of RECK mRNA through inactivation of ERK1/2. Cells were treated with the indicated concentrations of 3-bromoacetamino-4-methoxy-benzoylurea or 2.5 μmol/l U0126 for 24 h. (a) RECK mRNA was detected by real time reverse transcription–polymerase chain reaction and GAPDH served as a loading control. (b and c) Phospho-ERK1/2 (p-ERK1/2) and total ERK1/2 were detected by western blot and β-actin served as a loading control. GAPDH, glyceraldehyde-3-phosphate dehydrogenase.

shown that the stimulated expression of RECK significantly caused downregulation of MMP-2 and MMP-9 activities [31–35]. In this study, the expression of RECK mRNA was examined by RT-PCR. The results showed that HT-1080 cells expressed a low level of RECK mRNA (Fig. 8a). However, the expression of RECK mRNA was dose-dependently upregulated in F13-treated HT-1080 cells (Fig. 8a).

Earlier studies have implied that the ERK1/2 signalling pathway negatively regulates RECK expression [36–38]. We therefore assessed the phosphorylations of ERK1/2 by western blot. The phosphorylations of ERK1/2 were dramatically decreased by F13 in a dose-dependent manner (Fig. 8b). This said, the protein levels of total ERK1/2 were unchanged. Furthermore, the highly selective MEK1/2 inhibitor, U0126, led to the inhibition of phosphorylated activations of ERK1/2 in HT-1080 cells (Fig. 8c). U0126 also efficiently increased the expression of RECK (Fig. 8a). These results indirectly showed that F13 upregulated the expression of RECK through the ERK1/2 signalling pathway.

Discussion

It is well recognized that the development of tumor metastasis is a major cause of death in many human cancers. Tumor metastasis consists of numerous processes, including migration, adhesion to ECM, invasion into surrounding tissues, release from the primary tumor, intravasation, adhesion to vascular walls, extravasation, and formation of new foci [39]. In this study, we report that a novel benzoylurea derivative, F13, exerts inhibitions on the proliferation, migration, invasion and adhesion of human fibrosarcoma cells, HT-1080, in a dose-dependent manner. Over 1 μg/ml, F13 inhibited proliferation and induced apoptosis. At subtoxic concentrations (≤ 1 μg/ml), F13 could inhibit migration, invasion and adhesion. In an animal model, F13 also markedly inhibited the growth of mouse hepatoma, H22, up to 45% at a tolerant dose of 40 mg/kg (data not shown). The data suggest that F13 may disturb multiple stages of cancer development, and the role of F13 in the reduction of cell growth, migration and invasion at subtoxic doses is of considerable interest.

During the process of malignant progression, the migration of cells into the underlying extracellular matrices is a fundamental feature of tumor invasion. MMPs are a key family of proteolytic enzymes that are involved in tumor invasion, metastasis, and angiogenesis in cancer [40,41]. Inhibition of MMPs is regarded as a rational approach to metastatic disease therapy [42]. Type IV collagenases, MMP-2/9, the main members of MMP family, play an important role in cancer invasion and metastasis. Our data showed that F13 inhibited cell migration and invasion, and downregulated the activities of MMP-2/9 in the supernatant. This result reinforces earlier findings that inhibitors of MMP-2/9 significantly suppressed tumor metastasis in experimental animals [43] and stimulation of MMP secretion is associated with upregulated invasion [44].

The RECK gene was isolated as a transformation suppressor gene by using an expression cloning strategy designed to identify human cDNA-inducing flat reversion in a v-Ki-ras-transformed NIH3T3 cell line [45–47]. The gene encodes a membrane-anchored glycoprotein, which inhibits the activities of at least three MMP members, including MMP-2, MMP-9, and MT1-MMP, and inhibits tumor angiogenesis and metastasis [30,31,36,48,49]. Although RECK mRNA is highly expressed in most of human tissues and untransformed cells, it is downregulated or undetectable in many tumor cell lines or in cells expressing active oncogenes [31]. As the levels of MMP-2/9 mRNA were unchangeable as determined by qRT-PCR, the decrease in MMP-2/9 activities must be the result of a posttranscriptional event. The results (Fig. 8a) showed that F13 dramatically upregulated the expression of RECK mRNA in HT-1080 cells, consistent with the downregulation of MMP-2/9.

Earlier studies showed that the restored expression of RECK in malignant cells resulted in the suppression of invasive activity with concomitant decrease in the secretion of MMPs [29,31,33]. RECK negatively regulates MMP-9 in two ways: suppression of MMP-9 secretion from the cells and direct inhibition of its enzymatic activity [31]. RECK also inhibits the enzymatic activity of membrane-type 1 matrix metalloproteinase and MMP-2, resulting in reduced production of active MMP-2 [30]. These studies support our speculation that F13 inhibits MMP-2/9 activities through the induction of RECK to suppress invasion.

Earlier research has also shown that the HER-2/neu or ras oncogene transcriptionally represses RECK expression through inducing ERK activation [37,38]. Furthermore, LMP1 inhibits RECK expression through the ERK/Sp1 signalling pathway [36]. In this study, F13 suppressed the activation of the ERK signalling pathway while simultaneously upregulating RECK. Interestingly, the MEK1 and MEK2 selective inhibitor, U0126, also increased the expression of RECK in HT-1080 cells. Our data are consistent with an earlier report that inhibition of ERK activity attenuated MMP-9 activity and cell invasion [36]. Although the detailed mechanism inducing downregulation of RECK is not yet clear, the ERK signalling pathway seems to play a pivotal role in the regulation of RECK expression.

In conclusion, the benzoylurea derivative F13 dose-dependently exerts multiple anticancer effects: induction of apoptosis and inhibitions of cell proliferation, migration, adhesion and invasion. F13-mediated inhibition was associated with the inactivation of MMP2/9 by the induction of RECK expression, which was regulated by downregulation of the ERK signalling pathway. F13 might be a lead compound of RECK inducer for the development of new anticancer agents.

Acknowledgement

This project was supported by the grants from NSFC (No. 30772583), the National 973 Program (No. 2009CB521807). The authors thank Nicholas Coman and Kristy Miskimen for modifications of the writings.

References

1 Baud V, Karin M. Is NF-kappaB a good target for cancer therapy? Hopes and pitfalls. *Nat Rev Drug Discov* 2009; **8**:33–40.
2 Aggarwal BB, Shishodia S, Takada Y, Banerjee S, Newman RA, Bueso-Ramos CE, Price JE. Curcumin suppresses the paclitaxel-induced nuclear factor-kappaB pathway in breast cancer cells and inhibits lung metastasis of human breast cancer in nude mice. *Clin Cancer Res* 2005; **11**:7490–7498.
3 Shao RG, Zhen YS. Enediyne anticancer antibiotic lidamycin: chemistry, biology and pharmacology. *Anticancer Agents Med Chem* 2008; **8**:123–131.
4 Kunnumakkara AB, Anand P, Aggarwal BB. Curcumin inhibits proliferation, invasion, angiogenesis and metastasis of different cancers through interaction with multiple cell signaling proteins. *Cancer Lett* 2008; **269**:199–225.
5 Chen L, Jiang J, Cheng C, Yang A, He Q, Li D, Wang Z. P53 dependent and independent apoptosis induced by lidamycin in human colorectal cancer cells. *Cancer Biol Ther* 2007; **6**:965–973.
6 He QY, Liang YY, Wang DS, Li DD. Characteristics of mitotic cell death induced by enediyne antibiotic lidamycin in human epithelial tumor cells. *Int J Oncol* 2002; **20**:261–266.
7 Jiang B, Li DD, Zhen YS. Induction of apoptosis by enediyne antitumor antibiotic C1027 in HL-60 human promyelocytic leukemia cells. *Biochem Biophys Res Commun* 1995; **208**:238–244.
8 Liang YX, Zhang W, Li DD, Liu HT, Gao P, Sun YN, Shao RG. Mitotic cell death in BEL-7402 cells induced by enediyne antibiotic lidamycin is associated with centrosome overduplication. *World J Gastroenterol* 2004; **10**:2632–2636.
9 Sugimoto Y, Otani T, Oie S, Wierzba K, Yamada Y. Mechanism of action of a new macromolecular antitumor antibiotic, C-1027. *J Antibiot (Tokyo)* 1990; **43**:417–421.
10 Cobuzzi RJ Jr, Kotsopoulos SK, Otani T, Beerman TA. Effects of the enediyne C-1027 on intracellular DNA targets. *Biochemistry* 1995; **34**:583–592.
11 Liu X, He H, Feng Y, Zhang M, Ren K, Shao R. Difference of cell cycle arrests induced by lidamycin in human breast cancer cells. *Anticancer Drugs.* 2006; **17**:173–179.
12 Chen J, Ouyang ZG, Zhang SH, Zhen YS. Down-regulation of the nuclear factor-kappaB by lidamycin in association with inducing apoptosis in human pancreatic cancer cells and inhibiting xenograft growth. *Oncol Rep* 2007; **17**:1445–1451.
13 Liu X, Bian C, Ren K, Jin H, Li B, Shao RG. Lidamycin induces marked G2 cell cycle arrest in human colon carcinoma HT-29 cells through activation of p38 MAPK pathway. *Oncol Rep* 2007; **17**:597–603.
14 Zhen H, Xue Y, Zhen Y. Inhibition of angiogenesis by antitumor antibiotic C1027 and its effect on tumor metastasis. *Zhonghua Yi Xue Za Zhi* 1997; **77**:657–660.
15 Chen HW, Lee JY, Huang JY, Wang CC, Chen WJ, Su SF, *et al.* Curcumin inhibits lung cancer cell invasion and metastasis through the tumor suppressor HLJ1. *Cancer Res* 2008; **68**:7428–7438.
16 Donehower RC, Rowinsky EK. An overview of experience with TAXOL (paclitaxel) in the USA. *Cancer Treat Rev* 1993; **19** (**Suppl C**): 63–78.
17 Jordan MA, Wilson L. Microtubules and actin filaments: dynamic targets for cancer chemotherapy. *Curr Opin Cell Biol* 1998; **10**:123–130.
18 Rowinsky EK, Donehower RC. The clinical pharmacology and use of antimicrotubule agents in cancer chemotherapeutics. *Pharmacol Ther* 1991; **52**:35–84.
19 Song DQ, Wang YM, Du NN, He WY, Chen KL, Wang GF, *et al.* Synthesis and activity evaluation of benzoylurea derivatives as potential antiproliferative agents. *Bioorg Med Chem Lett* 2009; **19**:755–758.
20 Song DQ, Wang Y, Wu LZ, Yang P, Wang YM, Gao LM, *et al.* Benzoylurea derivatives as a novel class of antimitotic agents: synthesis, anticancer activity, and structure–activity relationships. *J Med Chem* 2008; **51**:3094–3103.
21 Song DQ, Du NN, Wang YM, He WY, Jiang EZ, Cheng SX, *et al.* Synthesis and activity evaluation of phenylurea derivatives as potent antitumor agents. *Bioorg Med Chem* 2009; **17**:3873–3878.
22 Jiang JD, Davis AS, Middleton K, Ling YH, Perez-Soler R, Holland JF, Bekesi JG. 3-(Iodoacetamido)-benzoylurea: a novel cancericidal tubulin ligand that inhibits microtubule polymerization, phosphorylates bcl-2, and induces apoptosis in tumor cells. *Cancer Res* 1998; **58**:5389–5395.
23 Jiang JD, Denner L, Ling YH, Li JN, Davis A, Wang Y, *et al.* Double blockade of cell cycle at g(1)-s transition and m phase by 3-iodoacetamido benzoyl ethyl ester, a new type of tubulin ligand. *Cancer Res* 2002; **62**:6080–6088.
24 Li JN, Song DQ, Lin YH, Hu QY, Yin L, Bekesi G, *et al.* Inhibition of microtubule polymerization by 3-bromopropionylamino benzoylurea (JIMB01), a new cancericidal tubulin ligand. *Biochem Pharmacol* 2003; **65**:1691–1699.
25 Rubinstein LV, Shoemaker RH, Paull KD, Simon RM, Tosini S, Skehan P, *et al.* Comparison of in vitro anticancer-drug-screening data generated with a tetrazolium assay versus a protein assay against a diverse panel of human tumor cell lines. *J Natl Cancer Inst* 1990; **82**:1113–1118.
26 Garbisa S, Sartor L, Biggin S, Salvato B, Benelli R, Albini A. Tumor gelatinases and invasion inhibited by the green tea flavanol epigallocatechin-3-gallate. *Cancer* 2001; **91**:822–832.
27 Ren K, Jin H, Bian C, He H, Liu X, Zhang S, *et al.* MR-1 modulates proliferation and migration of human hepatoma HepG2 cells through myosin

light chains-2 (MLC2)/focal adhesion kinase (FAK)/Akt signaling pathway. *J Biol Chem* 2008; **283**:35598–35605.
28 Sun HX, He HW, Zhang SH, Liu TG, Ren KH, He QY, Shao RG. Suppression of N-Ras by shRNA-expressing plasmid increases sensitivity of HepG2 cells to vincristine-induced growth inhibition. *Cancer Gene Ther* 2009; **16**:693–702.
29 Noda M, Oh J, Takahashi R, Kondo S, Kitayama H, Takahashi C. RECK: a novel suppressor of malignancy linking oncogenic signaling to extracellular matrix remodeling. *Cancer Metastasis Rev* 2003; **22**:167–175.
30 Oh J, Takahashi R, Kondo S, Mizoguchi A, Adachi E, Sasahara RM, *et al*. The membrane-anchored MMP inhibitor RECK is a key regulator of extracellular matrix integrity and angiogenesis. *Cell* 2001; **107**:789–800.
31 Takahashi C, Sheng Z, Horan TP, Kitayama H, Maki M, Hitomi K, *et al*. Regulation of matrix metalloproteinase-9 and inhibition of tumor invasion by the membrane-anchored glycoprotein RECK. *Proc Natl Acad Sci U S A* 1998; **95**:13221–13226.
32 Oh J, Seo DW, Diaz T, Wei B, Ward Y, Ray JM, *et al*. Tissue inhibitors of metalloproteinase 2 inhibits endothelial cell migration through increased expression of RECK. *Cancer Res* 2004; **64**:9062–9069.
33 Liu LT, Chang HC, Chiang LC, Hung WC. Histone deacetylase inhibitor up-regulates RECK to inhibit MMP-2 activation and cancer cell invasion. *Cancer Res* 2003; **63**:3069–3072.
34 Kato K, Long NK, Makita H, Toida M, Yamashita T, Hatakeyama D, *et al*. Effects of green tea polyphenol on methylation status of RECK gene and cancer cell invasion in oral squamous cell carcinoma cells. *Br J Cancer* 2008; **99**:647–654.
35 Simizu S, Takagi S, Tamura Y, Osada H. RECK-mediated suppression of tumor cell invasion is regulated by glycosylation in human tumor cell lines. *Cancer Res* 2005; **65**:7455–7461.
36 Liu LT, Peng JP, Chang HC, Hung WC. RECK is a target of Epstein–Barr virus latent membrane protein 1. *Oncogene* 2003; **22**:8263–8270.
37 Chang HC, Cho CY, Hung WC. Silencing of the metastasis suppressor RECK by RAS oncogene is mediated by DNA methyltransferase 3b-induced promoter methylation. *Cancer Res* 2006; **66**:8413–8420.
38 Hsu MC, Chang HC, Hung WC. HER-2/neu represses the metastasis suppressor RECK via ERK and Sp transcription factors to promote cell invasion. *J Biol Chem* 2006; **281**:4718–4725.
39 Woodhouse EC, Chuaqui RF, Liotta LA. General mechanisms of metastasis. *Cancer* 1997; **80**:1529–1537.
40 Westermarck J, Kahari VM. Regulation of matrix metalloproteinase expression in tumor invasion. *FASEB J* 1999; **13**:781–792.
41 Chang C, Werb Z. The many faces of metalloproteases: cell growth, invasion, angiogenesis and metastasis. *Trends Cell Biol* 2001; **11**:S37–S43.
42 Elkin M, Reich R, Nagler A, Aingorn E, Pines M, De-Groot N, *et al*. Inhibition of matrix metalloproteinase-2 expression and bladder carcinoma metastasis by halofuginone. *Clin Cancer Res* 1999; **5**:1982–1988.
43 Hidalgo M, Eckhardt SG. Development of matrix metalloproteinase inhibitors in cancer therapy. *J Natl Cancer Inst* 2001; **93**:178–193.
44 Kim MS, Kwak HJ, Lee JW, Kim HJ, Park MJ, Park JB, *et al*. 17-Allylamino-17-demethoxygeldanamycin down-regulates hyaluronic acid-induced glioma invasion by blocking matrix metalloproteinase-9 secretion. *Mol Cancer Res* 2008; **6**:1657–1665.
45 Noda M, Kitayama H, Matsuzaki T, Sugimoto Y, Okayama H, Bassin RH, Ikawa Y. Detection of genes with a potential for suppressing the transformed phenotype associated with activated ras genes. *Proc Natl Acad Sci U S A* 1989; **86**:162–166.
46 Kitayama H, Sugimoto Y, Matsuzaki T, Ikawa Y, Noda M. A ras-related gene with transformation suppressor activity. *Cell* 1989; **56**:77–84.
47 Takahashi C, Akiyama N, Matsuzaki T, Takai S, Kitayama H, Noda M. Characterization of a human MSX-2 cDNA and its fragment isolated as a transformation suppressor gene against v-Ki-ras oncogene. *Oncogene* 1996; **12**:2137–2146.
48 Sasahara RM, Brochado SM, Takahashi C, Oh J, Maria-Engler SS, Granjeiro JM, *et al*. Transcriptional control of the RECK metastasis/angiogenesis suppressor gene. *Cancer Detect Prev* 2002; **26**:435–443.
49 Sternlicht MD, Werb Z. How matrix metalloproteinases regulate cell behavior. *Annu Rev Cell Dev Biol* 2001; **17**:463–516.